Supporting Information

A luminescent metal-organic framework with tetragonal nanochannel as efficient chemosensor for nitroaromatic explosives detection

Wei Xie,[a] Wei Jiang,[a] Guang-Juan Xu,[a] Shu-Ran Zhang,[a] Yan-Hong Xu,*[a] and Zhong-Min Su*[b]

[a] Key Laboratory of Preparation and Application of Environmental Friendly Materials (Jilin Normal University), Ministry of Education, Changchun, 130103, China.

E-mail: xuyh198@163.com

[b] Institute of Functional Material Chemistry, Faculty of Chemistry, Northeast Normal University, Changchun 130024, Jilin (P. R. China).

E-mail: zmsu@nenu.edu.cn

S1. Materials and measurements

All chemical reagents for synthesis were purchased commercially and were used directly without further purification. Powder X-ray diffraction (PXRD) patterns were performed on a Rigaku model RINT Ultima III diffractometer in the range of 3 - 50° with 0.02° increment at room temperature. The fourier transformed infrared spectroscopy (FT-IR) spectra were recorded in the range 4000-400 cm^{-1} on a Perkin-elmer model FT-IR-frontier infrared spectrometer using KBr pellets. Thermogravimetric analysis (TGA) was performed using a Q5000IR analyser (TA Instruments) with an automated vertical overhead thermobalance heated from room temperature to 700 ºC at a ramp rate of 5 °C/min under nitrogen gas atmosphere. Elemental analyses (C, H and N) were conducted on a Perkin-Elmer 2400CHN elemental analyzer. The solid UV-visible analyzer was performed using Jasco UV-770. The fluorescence spectra were carried out using Jasco FP-8600 spectrometer (JAPAN) spectrofluorometer.

S2. Synthesis of MOF 1

$Zn(NO_3)_2 \cdot 6H_2O$ (0.06 g, 0.2 mmol) and 4,4',4''-nitrilotribenzoic acid (H_3TPA, 0.0151 g, 0.040 mmol) were dissolved in 6 mL DMA (N, N-dimethylacetamide), and then the final mixture was placed into a Teflon-lined stainless steel vessel (15 mL) under autogenous pressure and heated at 100 ℃ for 3 days, and thereafter was slowly cooled to room temperature. Light yellow block crystals were obtained, which were washed with mother liquid, in about 62 % yield based on H_3TPA. Elemental microanalysis for $C_{74}H_{100}N_{10}O_{23}Zn_4$, calculated (%): C, 50.53; H, 5.73; N, 7.96. Found (%): C, 50.87; H, 5.69; N, 7.53. IR (KBr, cm^{-1}): 3436.84 (w), 2937.61 (w), 2878.46 (w), 1673.49 (s), 1594.76 (s), 1562.83 (w), 1403.45 (s), 1384.79 (s), 1313.89 (m), 1267.24 (m), 1174.51 (m), 783.46 (m).

S3. Single-crystal X-ray diffraction

Single-crystal X-ray diffraction data for MOF **1** in this work were recorded by using a Bruker Apex CCD diffractometer with graphite-monochromated Mo-Kα radiation (λ = 0.71069 Å) at 293 K. All non-hydrogen atoms were refined with anisotropic displacement parameters and hydrogen positions were fixed at calculated positions and refined isotropically. Absorption corrections were applied using multi-scan technique. All the structures were solved by Direct Method and refined by full-matrix least-squares techniques using the SHELXL-2018 program[1] within WINGX software. All the solvent molecules which are highly disordered and not able to be modeled were treated by the SQUEEZE[2] routine in PLATON[3]. Thus, all of electron densities from free solvent molecules have been "squeezed" out.

The detailed crystallographic data and structure refinement parameters for **1** summarized in Table S1. CCDC for **1**: 2044116.

Table S1. Crystal data and structure refinements for MOF **1**.

Identification code	**1**
formula	$C_{74}H_{100}N_{10}O_{23}Zn_4$
Formula weight	1759.15
Crystal system	Monoclinic
Space group	$P2_1/c$
a (Å)	24.677 (5)
b (Å)	21.780 (5)
c (Å)	25.025 (5)
α (°)	90.00
β (°)	109.500 (5)
γ (°)	90.00
V (Å^3)	12679 (5)
Z	4
$D_{calcd.}$[g cm^{-3}]	0.554
F(000)	2120.0
Reflections collected	72906 / 22317
R(int)	0.0980
Goodness-of-fit on F^2	0.718
$R_1{}^a$ [I>2σ (I)]	0.0578
$wR_2{}^b$	0.1774

$^aR_1 = \Sigma||F_o| - |F_c||/\Sigma|F_o|$, $^bwR_2 = |\Sigma w(|F_o|^2-|F_c|^2)|/\Sigma|w(F_o^2)^2|^{1/2}$.

S4. MOF 1 sensing small solvent molecules

The solvent sensing experiments have been performed as follows: finely ground samples of **1** (5 mg) were immersed in different solvents (3 mL), treated by ultrasonication, and then aged to form stable emulsions before fluorescence were measured.

The fluorescence quenching was analyzed using the Stern-Volmer equations:

$$I_0/I = 1 + K_{sv}[Q]$$

where I_0 and I are the fluorescence intensities, in the absence and presence of analyte, respectively, K_{sv} is the Stern-Volmer quenching constant and [Q] is the concentration of analyte.

The limit of detection concentration (LOD) was calculated according to the formula:

$$LOD = 3\delta / Ksv$$

δ is the standard deviation of the detection method.

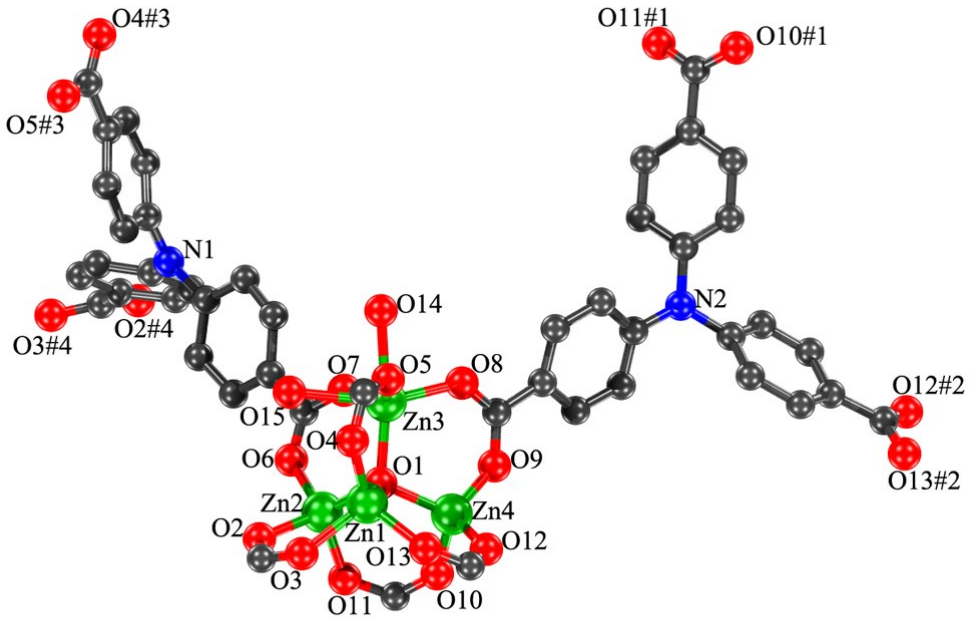

Fig. S1 The coordination modes of Zn^{2+} ions in **1,** symmetry codes: #1 x, -0.5-y, 0.5+z; #2 -x, -0.5+y, 0.5-z; #3 1-x, -y, 1-z; #4 1-x, -0.5+y, 0.5-z. All hydrogen atoms have been omitted for clarity. Green = Zn; dark gray = C; red = O; blue = N.

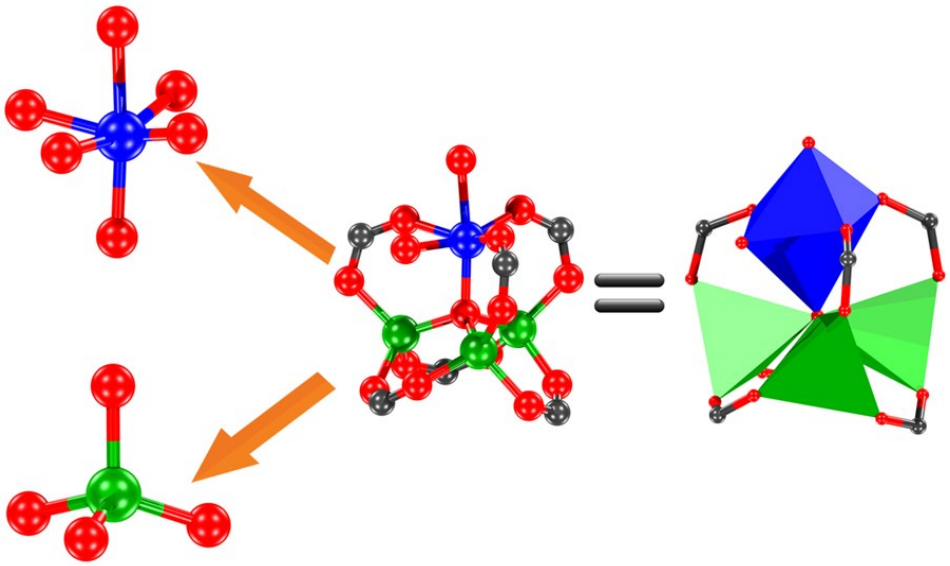

Fig. S2 The Zn_4O cluster SBU in **1.**

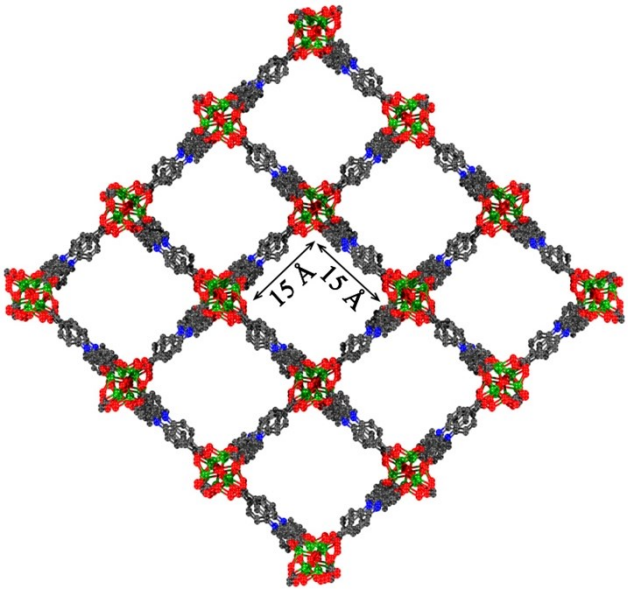

Fig. S3 Ball-and-stick representation of the 3D network of **1** viewed from the [101] direction and the channel (15 Å × 15 Å).

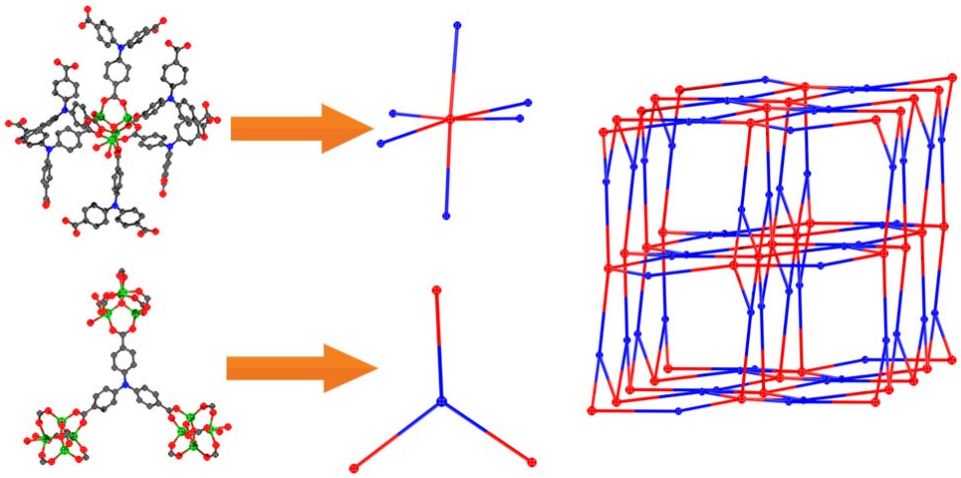

Fig. S4 The (3, 6)-connected topology network in **1**.

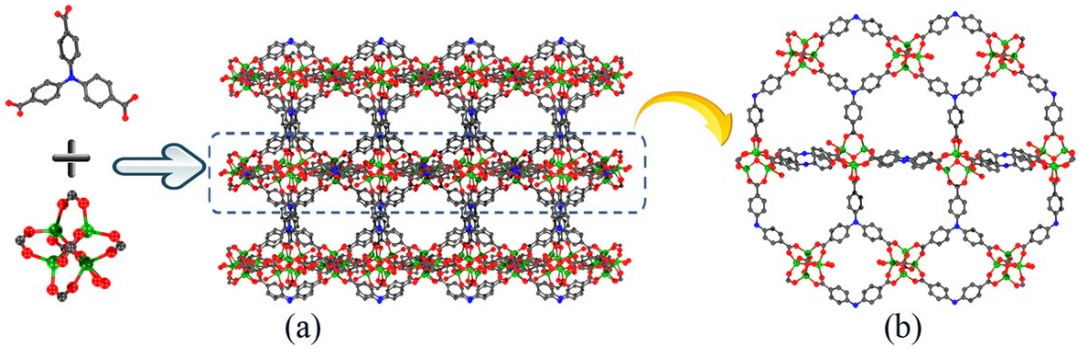

Fig. S5 (a) Ball-and-stick representations of the 3D structure of **1**. (b) The layer is formed by Zn_4O clusters and TPA^{3-} ligands.

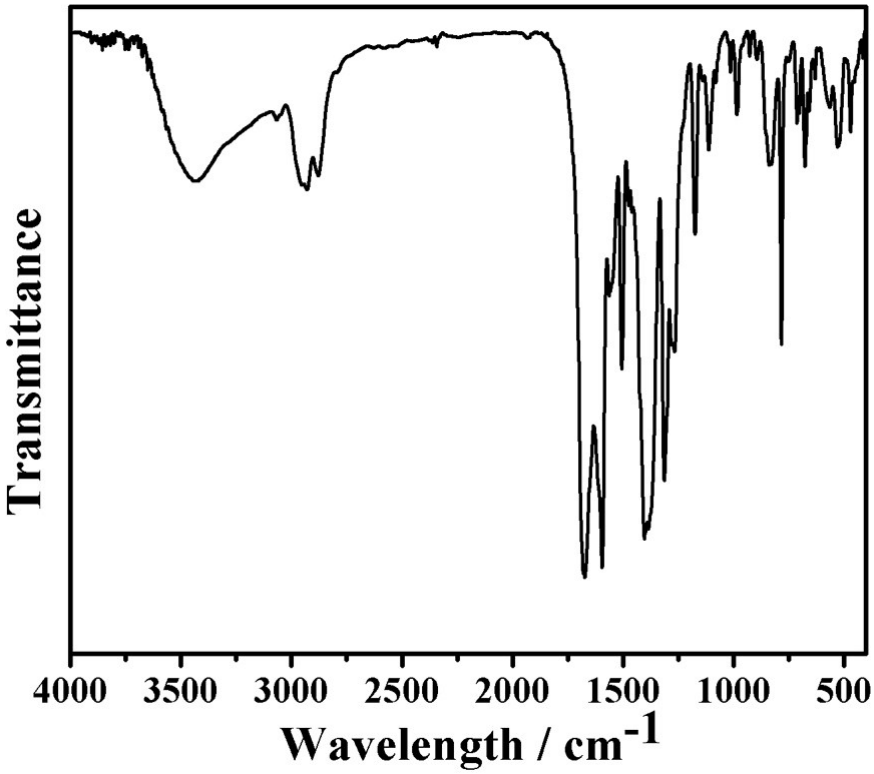

Fig. S6 The FT-IR curve of as-synthesized complex **1** at room temperature.

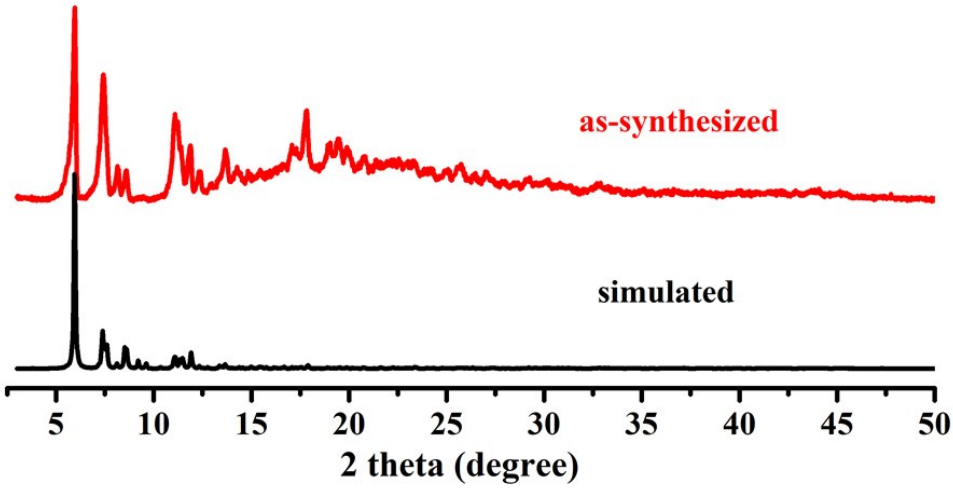

Fig. S7 X-ray powder diffraction patterns of simulated **1** and as-synthesized **1**.

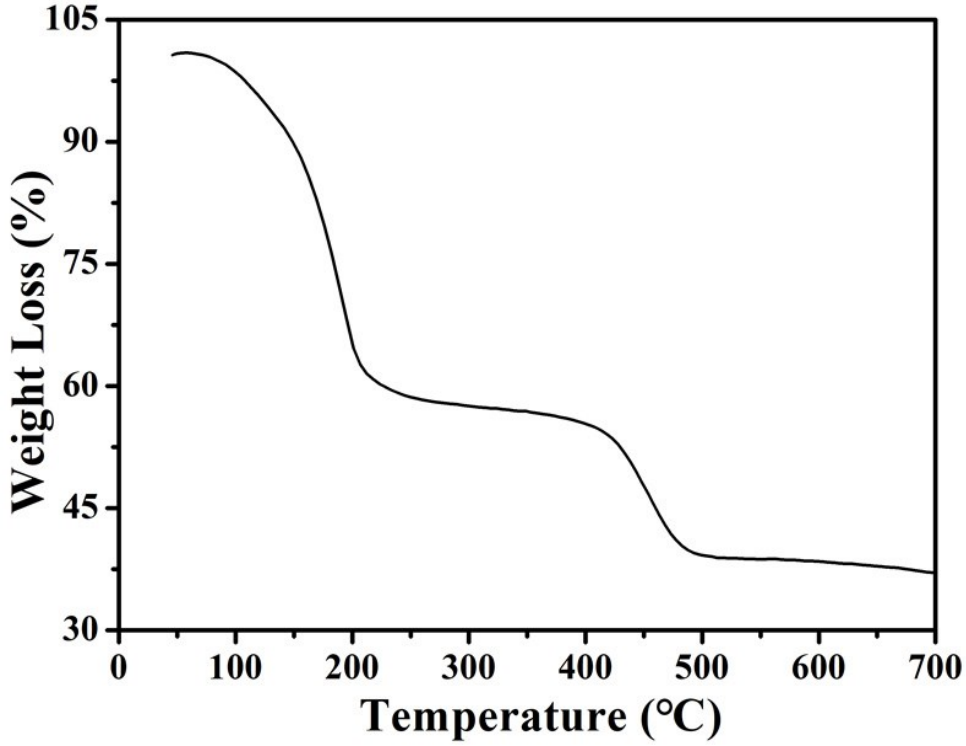

Fig. S8 TGA curve of as-synthesized MOF **1**.

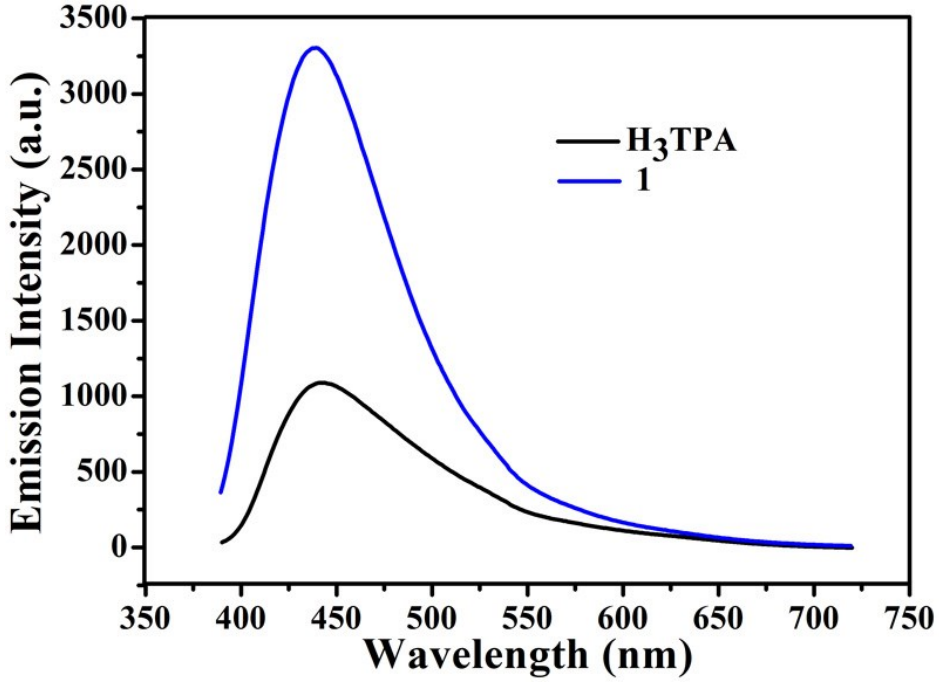

Fig. S9 Solid photoluminescence emission spectra of H_3TPA ligand and complex **1** (λ_{ex} = 365 nm) at room temperature.

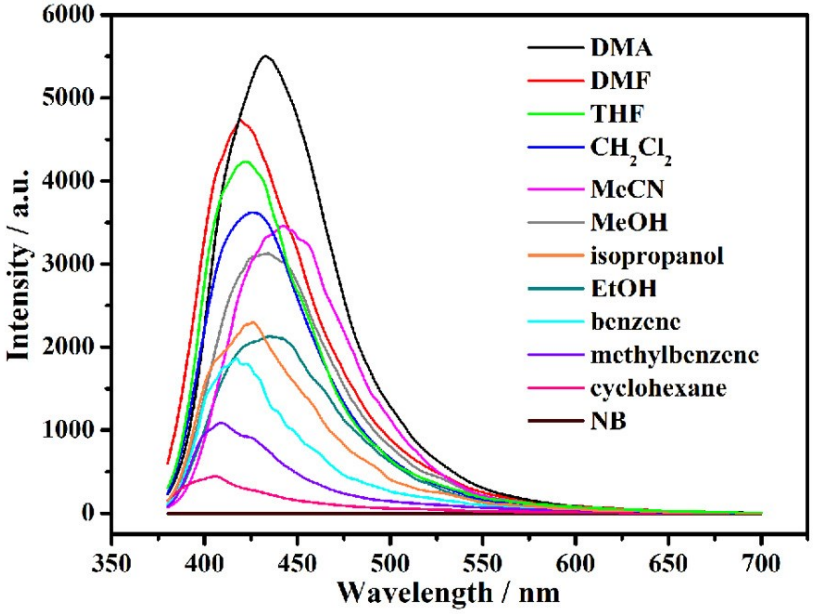

Fig. S10 The photoluminescence emission spectra of **1** in different solvents (λ_{ex} = 365 nm) at room temperature (solvents = DMF, DMA, MeOH, EtOH, isopropanol, CH_2Cl_2, MeCN, THF, benzene, methylbenzene, cyclohexane and NB).

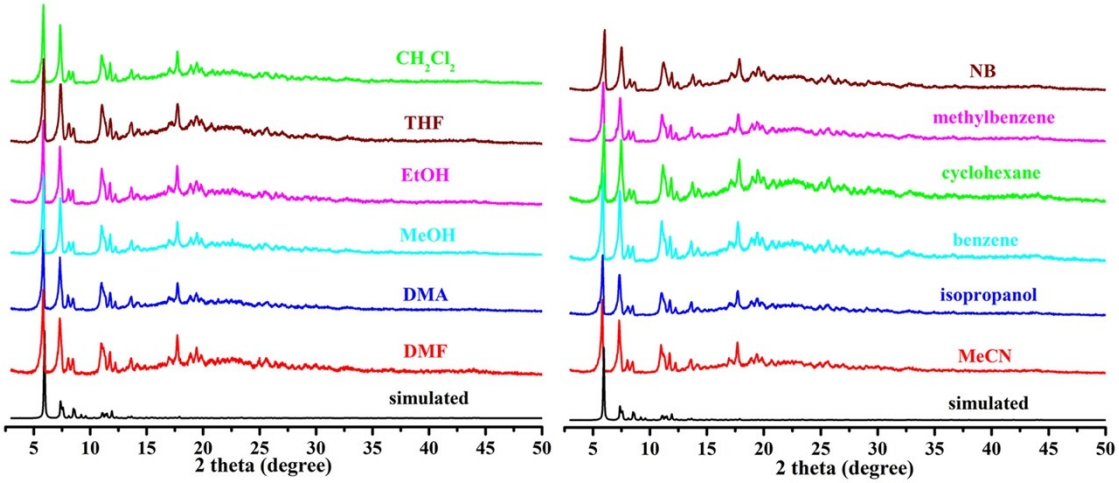

Fig. S11 The PXRDs of MOF **1** after solvents (solvents = DMF, DMA, MeOH, EtOH, THF, CH_2Cl_2, MeCN, isopropanol, benzene, cyclohexane, methylbenzene and NB) sensing.

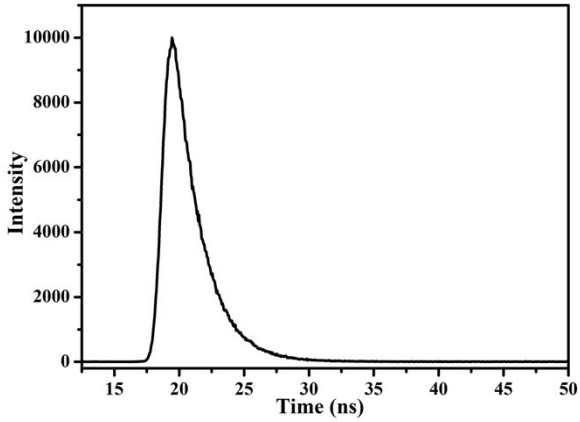

Fig. S12 The fluorescence decay of complex **1** in DMA emulsion.

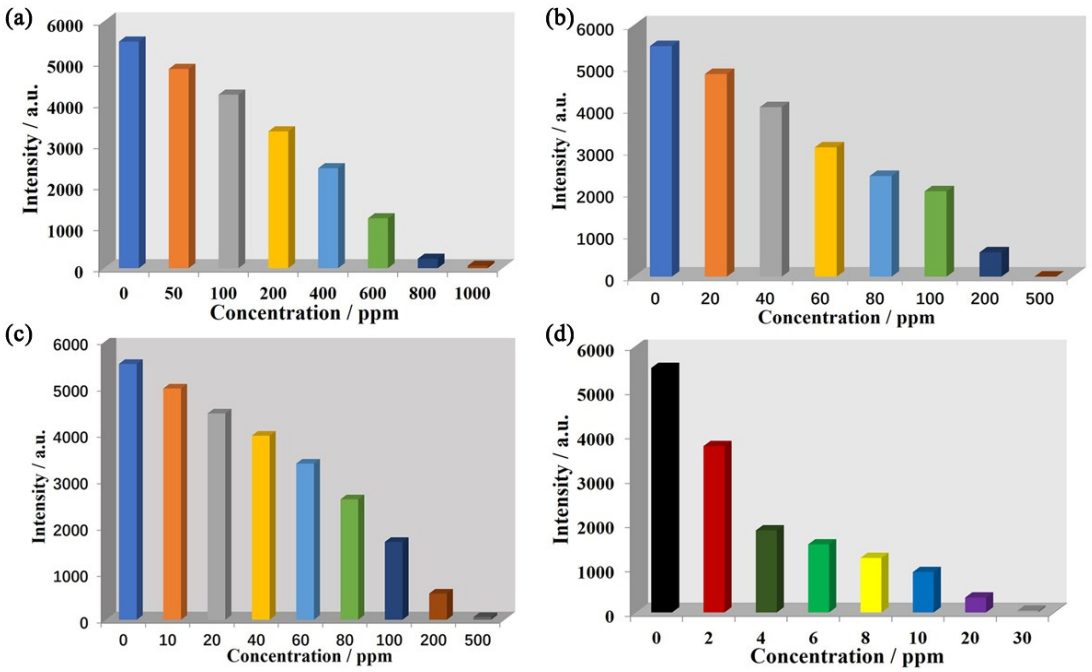

Fig. S13 The luminescent emission intensities of sample **1** in different concentrations of nitroaromatic explosives solutions (a) NB, (b) 1,2-DNB, (c) 1,3-DNB, and (d) PA respectively.

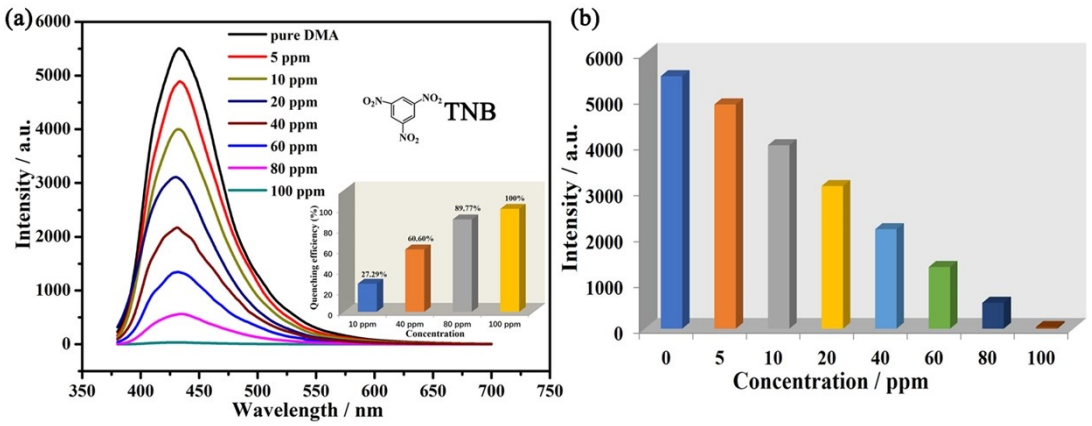

Fig. S14 (a) The fluorescence emission spectra of **1** in DMA solutions containing different concentrations of TNB, Inset: Corresponding luminescence quenching efficiency in selected concentrations of TNB, (b) The corresponding luminescent emission intensities of sample **1** in TNB solutions.

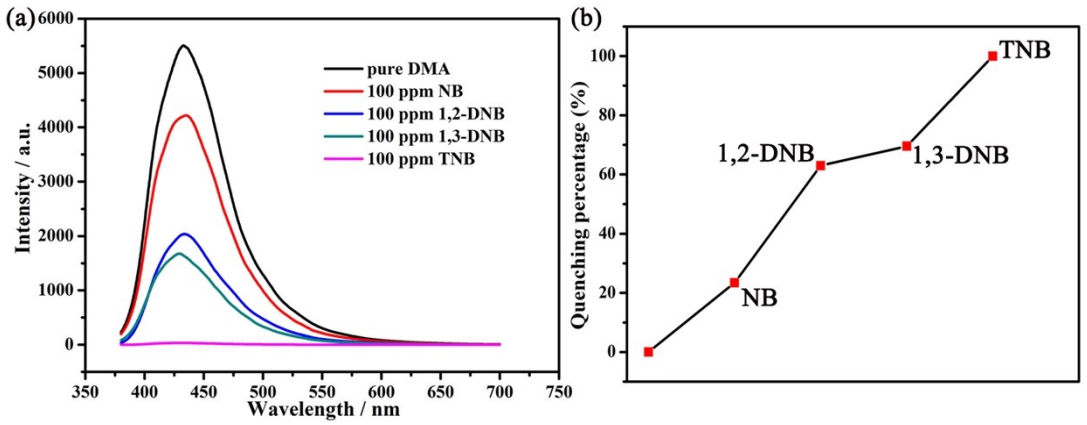

Fig. S15 (a) The luminescent emission spectra and (b) quenching efficiency of **1** in DMA solutions containing nitroaromatic explosives compounds (100 ppm). The quenching efficiency, defined by $(I_0\text{-}I)/I_0 \times 100\%$, where I_0 and I are the luminescence intensities of **1** before and after the addition of the analyte, respectively.

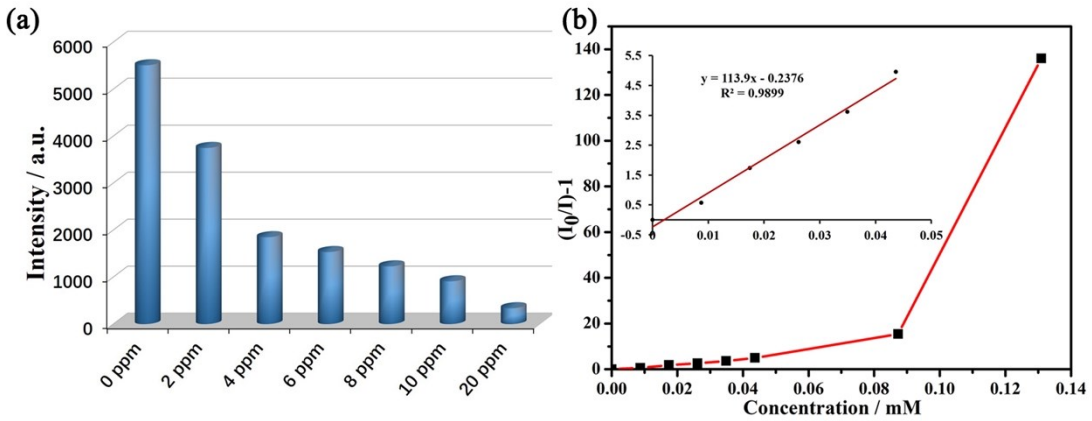

Fig. S16 (a) The emission intensities of **1** in DMA containing different amounts of PA and (b) corresponding Stern-Volmer plots of PA.

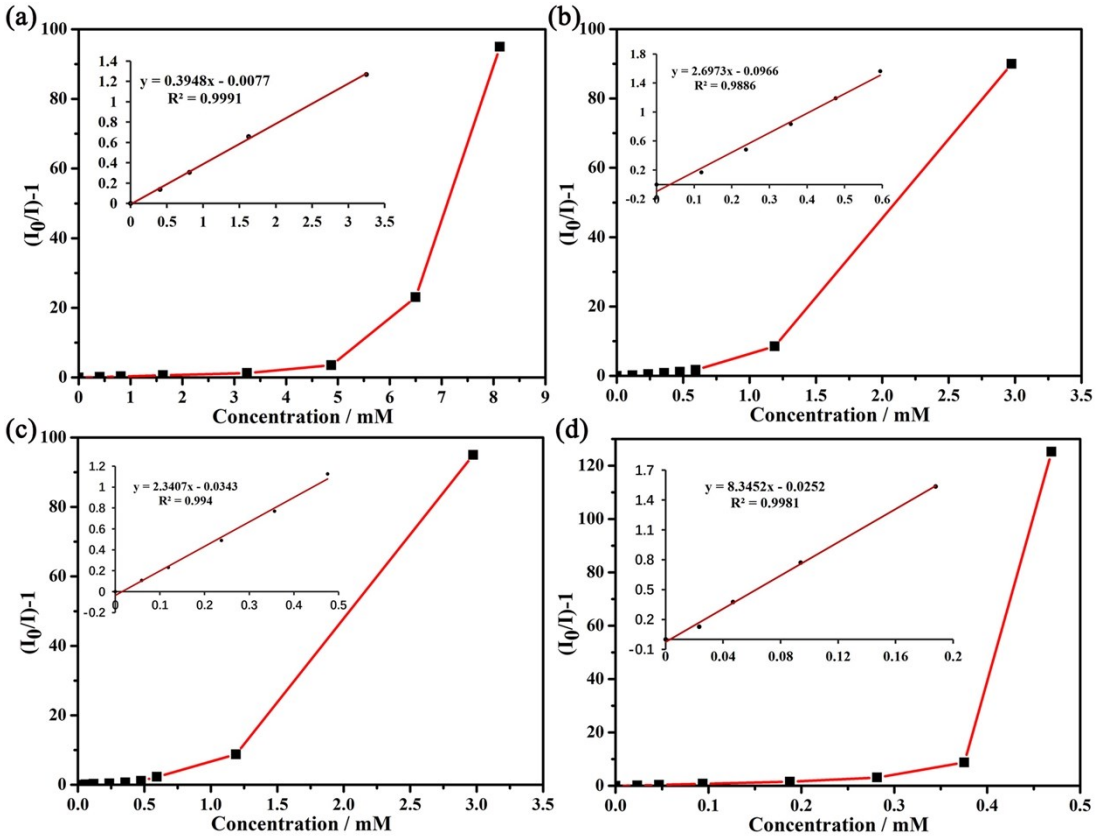

Fig. S17 The Stern-Volmer plots for (a) NB, (b) 1,2-DNB, (c) 1,3-DNB and (d) TNB (insert: the corresponding enlarged views of selected areas).

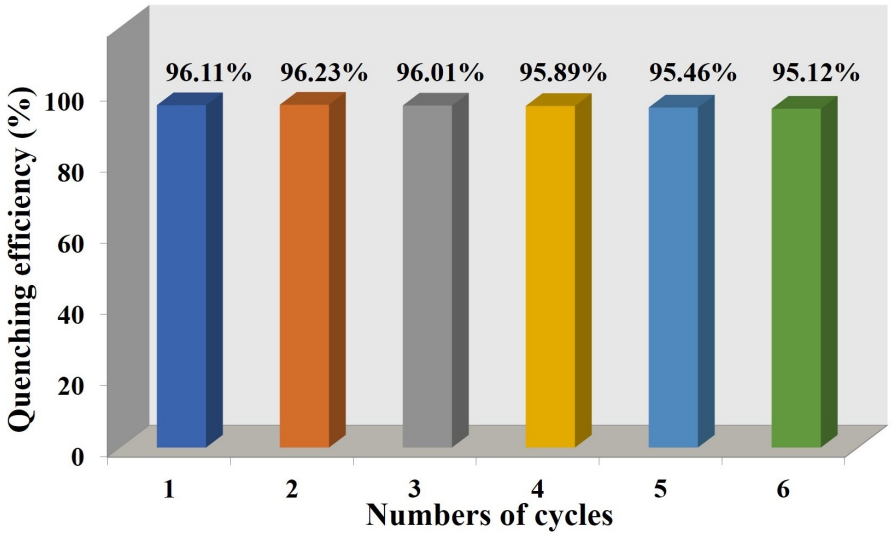

Fig. S18 Bar diagram depicting the recyclable quenching efficiency of **1** dispersed in 800 ppm NB solution over 6 cycles.

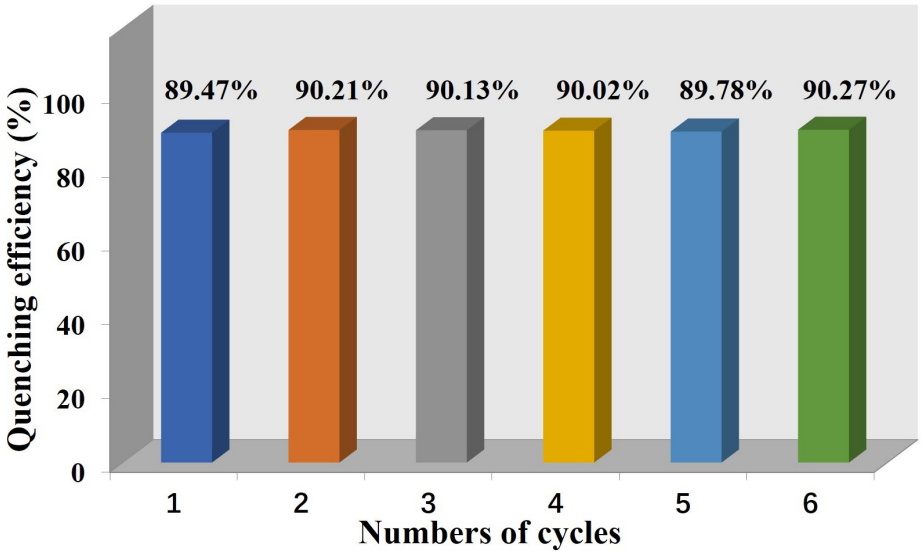

Fig. S19 Bar diagram depicting the recyclable quenching efficiency of **1** dispersed in 200 ppm 1,2-DNB solution over 6 cycles.

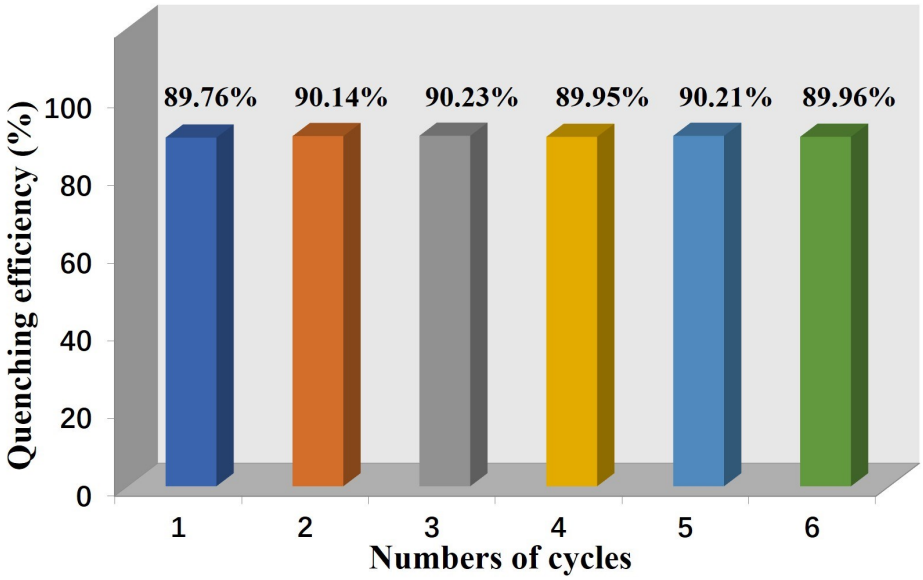

Fig. S20 Bar diagram depicting the recyclable quenching efficiency of **1** dispersed in 200 ppm 1,3-DNB solution over 6 cycles.

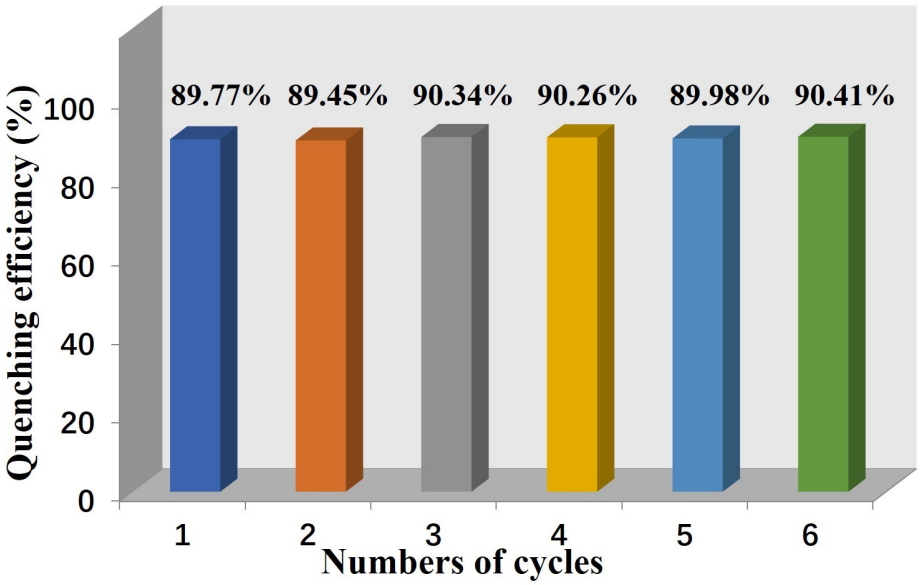

Fig. S21 Bar diagram depicting the recyclable quenching efficiency of **1** dispersed in 80 ppm TNB solution over 6 cycles.

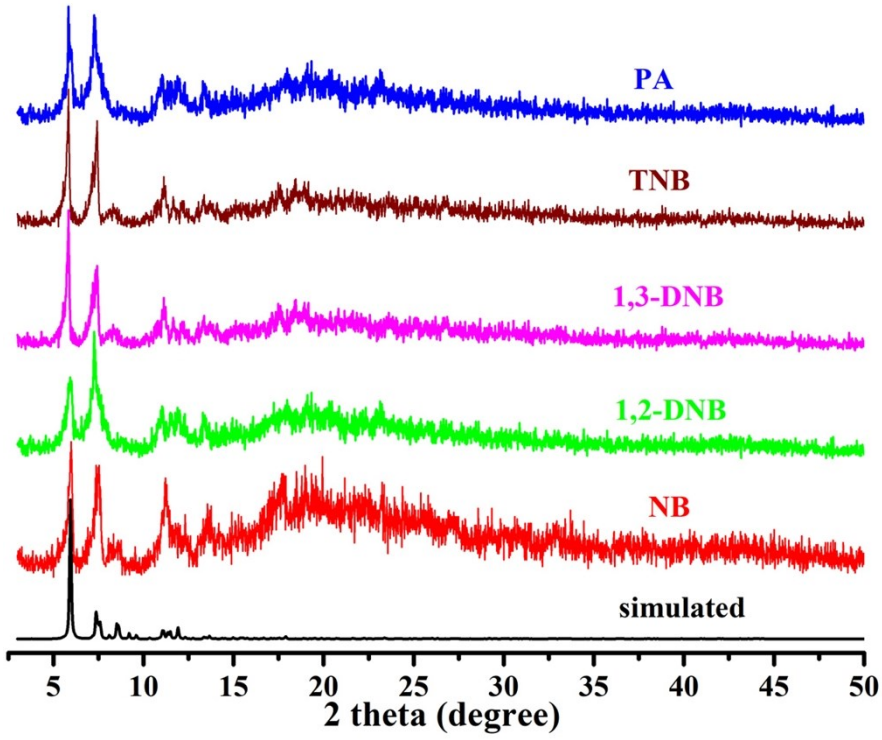

Fig. S22 The PXRD patterns of **1** after detection of NB, 1,2-DNB, 1,3-DNB, TNB and PA in DMA after cycle 6, respectively.

References:

[1] D. Leggas, O. V. Tsodikov, *Acta Cryst. A* 2015, **71**, 319-324.

[2] A. Spek, *Acta Cryst. C* 2015, **71**, 9-18.

[3] A. Spek, *Acta Cryst. D* 2009, **65**, 148-155.